

Metastability in the Two-Dimensional Ising Model

R. J. McCraw¹ and L. S. Schulman¹

Received June 9, 1977

Metastability in the Ising model is studied in two ways. In a dynamical Monte Carlo model, metastable magnetization and lifetime are measured for various magnetic fields and low temperatures. Following up a proposed relation between analytic continuation of transfer matrix eigenvalues and metastability, transfer matrix eigenvalues are studied. We examine the extent to which these approaches agree. The Monte Carlo data also provide quantitative support for the critical droplet model for decay.

KEY WORDS: Metastability; Ising model; transfer matrix; dynamic Ising model.

1. INTRODUCTION

There was recently proposed a relation between certain eigenvalues of the transfer matrix for the two-dimensional Ising model and metastability in that system.⁽¹⁾ Another approach to metastability is through a dynamical Ising model, using Monte Carlo techniques.⁽²⁻⁵⁾ We here present numerical calculations from both points of view, which show that the transfer matrix and Monte Carlo work address the same phenomenon. This supports the thesis of Ref. 1, namely the relevance of the transfer matrix to metastability. The structure of the transfer matrix eigenvalues, however, is more complicated than envisaged there and suggests that the first-order phase transition causes an essential singularity in the free energy (agreeing with other studies⁽⁶⁻⁹⁾).

Besides results concerning the transfer matrix, our systematic study of Monte Carlo decay times and magnetization at *low* temperatures T and "small" systems appears to be new. We find that the formula

$$\Gamma \sim (\text{volume}) \times \exp(-\phi/T) \quad (1)$$

describes a wide range of decay rates, where for low T , ϕ is close to the energy

¹ Physics Department, Indiana University, Bloomington, Indiana, and Physics Department, Technion, Haifa, Israel.

cost for certain stable state clusters in the metastable background, providing evidence for the role of critical droplets in decay.

We also find agreement, for small external field H , between the magnetization of the metastable state as predicted by (a) the transfer matrix, (b) the first few terms of the low-temperature expansion⁽¹⁰⁾ (used outside its region of known convergence), and (c) the dynamical Ising model (i.e., Monte Carlo results).

In Section 2 we discuss our work on the transfer matrix. The Monte Carlo results are presented in Section 3. Section 4 deals with some of the relations between these. Conclusions and remarks are presented in Section 5.

2. THE TRANSFER MATRIX APPROACH TO METASTABILITY

2.1. Notation and Review of the Model

According to Ref. 1, the metastable free energy is derived from the transfer matrix eigenvalue of largest "wrong" magnetization. We consider a periodic $N \times \infty$ lattice with Ising free energy

$$E = -J \sum_{\substack{\text{nearest} \\ \text{neighbor}}} \sigma\sigma - H \sum \sigma$$

where H is the external magnetic field and the spins $\sigma = \pm 1$. The interaction coefficient J will be taken equal to 1.

The associated $2^N \times 2^N$ symmetric transfer matrix L is defined as follows. For two column configurations $|\mu\rangle = (\sigma_1, \dots, \sigma_N)$ and $|\mu'\rangle = (\sigma'_1, \dots, \sigma'_N)$

$$\langle \mu | L | \mu' \rangle = \exp \left\{ \frac{\nu}{2} \sum_{i=1}^N (\sigma_i \sigma_{i+1} + \sigma'_i \sigma'_{i+1}) + \frac{1}{2} h \sum_{i=1}^N (\sigma_i + \sigma'_i) + \nu \sum_{i=1}^N \sigma_i \sigma'_i \right\} \quad (2)$$

where $\nu = J/T$ and $h = H/T$. Let $\lambda_j^{(N)}$ be the j th eigenvalue of L ($\lambda_0 > \lambda_1 > \lambda_2 > \dots$) and define the free energy associated with that eigenstate to be

$$F_j^{(N)} = -(T/N) \log \lambda_j^{(N)} \quad (3)$$

With this definition $\lim_{N \rightarrow \infty} F_0^{(N)}$ is the usual free energy. The magnetization m is the derivative of the free energy with respect to $-H$. In Ref. 1 it was proposed that the metastable free energy is $\lim_{N \rightarrow \infty} F_j^{(N)}$ for that eigenstate j with the largest magnetization opposite in direction to the magnetic field.

We have diagonalized the transfer matrix for $N = 5, 7, 9, 11$ for various values of H and T . In Fig. 1 the $N = 7$ free energy levels are shown for $T = 1$ (in our units $T_c = 2.269\dots$). We assume a magnetic field in the negative direction. The stable state has a magnetization of approximately -1 and the metastable state a magnetization near $+1$. These states are found to be

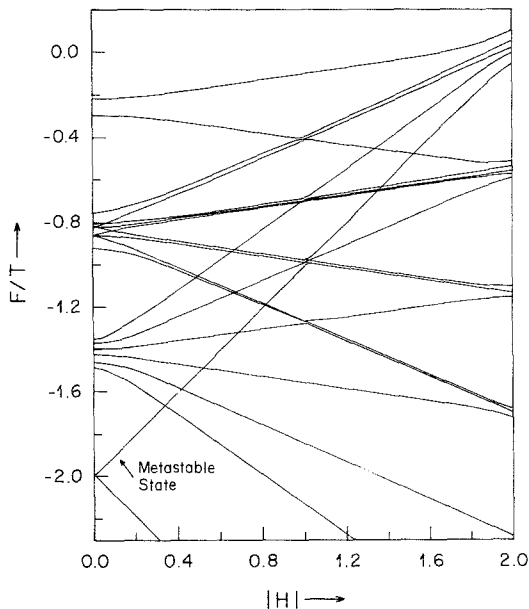


Fig. 1. Plot of (free energy)/ $T = -\log(\text{eigenvalue})/N$ for $2^7 \times 2^7$ transfer matrix for various eigenstates as a function of H for $T = 1$. Crossings are not accurately depicted.

almost purely composed of the vectors $(- - \dots - -)$ and $(+ + \dots + +)$, respectively. The other states can be similarly identified by their magnetization. In Fig. 1 only 20 energy levels are shown (rather than 2^7) because only translationally invariant states mix with the metastable state.² We have constructed the 20 translationally invariant states [there are $2 + (2^N - 2)/N$ such states for N prime] and diagonalized the restricted 20×20 transfer matrix to get our numerical results.

We introduce the following notation:

$$|0\rangle = (+ + \dots +) \quad \text{all } N \text{ spins} = +1 \quad (4)$$

This is the $T \rightarrow 0$ eigenfunction with the $T \rightarrow 0$ metastable state. Let

$$|xI\rangle = (+ + \dots + - - \dots - + + \dots +) \quad (5)$$

² Because L and the boundary conditions are translationally invariant and because variation of h can be considered a translationally invariant perturbation, the space of translationally invariant states will remain the same for all h . Since the stable ground state is translationally invariant, the metastable state, gotten by analytic continuation, shares this property. The translationally invariant space can be conveniently constructed by taking a basis and applying the operator $B = \sum_{j=1}^N A^j$ (where A is a translation operator) to all states and normalizing appropriately. The dimension of the translationally invariant subspace is computed by considering the number of basis vectors projected onto the same state by B .

For this state there are l consecutive $(-)$ spins, beginning at position x .

$$\begin{aligned} |0^*\rangle &\equiv [\text{the normalized translationally invariant} \\ &\quad \text{state associated with } |0\rangle] \\ &= |0\rangle \end{aligned} \tag{6}$$

$$\begin{aligned} |l^*\rangle &\equiv [\text{the normalized translationally invariant} \\ &\quad \text{state associated with any } |xl\rangle, \quad x = 1, \dots, N] \\ &= (1/\sqrt{N})[|1l\rangle + |2l\rangle + \dots + |Nl\rangle] \end{aligned} \tag{7}$$

The translationally invariant states are similarly defined for the other states. We write $|\mu^*\rangle$ as the translationally invariant state associated with $|\mu\rangle$. Away from the crossing regions most eigenvectors are composed predominantly of one such $|\mu^*\rangle$.

2.2. Numerical Results

For the purpose of establishing the relevance of transfer matrix eigenvalues to properties of the metastable state, the first satisfying feature to emerge from our numerical work is that as N varies, the metastable free energy changes little (cf. Table I). Although the label of the metastable level may change with N , there is always an eigenvector with the appropriate eigenvalue. This suggests that the metastable free energy has a thermodynamic limit. Only the stable state shares this property.

In Table II, the metastable free energy is compared with the free energy obtained by evaluation of the first few terms of the low-temperature expansion [up to $\mu^4 g_4(z)$ in the notation of Ref. 10] for $H < 0$, and for $T = 1$. (Presumably for $H < 0$ the series is an asymptotic expansion.) The magnetization is also shown. For low $|H|$ the low-temperature expansion and the transfer matrix are seen to agree very well. We have also checked $T = 1.25$ and $T = 0.714\dots$ ($\nu = 1.4$) and found similar results. The agreement is better for $T = 0.714\dots$ and worse for $T = 1.25$, as expected.

The values of H in Table II are chosen so as to be away from the regions where the metastable state crosses other energy levels (cf. Fig. 1). In these

Table I. Metastable Free Energy for Various N and H at $T = 1.0$

$-H$	$N = 5$	$N = 7$	$N = 9$	$N = 11$
0.1	-1.9004292157	-1.9004292179	-1.9004292179	-1.9004292179
0.3	-1.7006573235	-1.7006573445	-1.7006573404	-1.7006573403
0.9	-1.1030688848	-1.1030692876	-1.1030692860	-1.1030692860
1.5	-0.5086656612	-0.5086657017	-0.5086657018	-0.5086657018
1.9	-0.1395653130	-0.1396039301	-0.139606245	-0.1396064060

Table II. Metastable Free Energy and Magnetization from Transfer Matrix and Low-Temperature Expansion^a

$-H$	F (LT)	m (LT)	F (TM)	m (TM)
0	2.00034826	0.99928	2.00034828	0.99927
0.3	1.70065662	0.99858	1.70065734	0.99857
0.6	1.401287	0.99696	1.401317	0.99626
0.75	1.251862	0.99521	1.251798	0.99424
0.90	1.102807	0.99176	1.103069	0.98515
1.15	0.856628	0.97310	0.852532	0.98445
1.75	0.473	-0.62	0.270519	0.91939

^a To fourth order in $\exp(2|H|/T)$, for $T = 1.0$. Columns 2 and 3 are low-temperature (LT) expansion values for free energy and m , respectively, and columns 4 and 5 give the corresponding data for the transfer matrix (TM).

crossing regions the identification of the metastable state is more complicated than previously discussed. The reason is that the translationally invariant states “interact” with the metastable state when they cross as a function of H . The crossed lines are replaced by a hyperbola, so that a gap results between the free energy levels. The actual crossing occurs at two branch points in the complex H plane located symmetrically about the real H axis. Their distance from the real H axis, and consequently the size of the free energy gap for real H , is related to the transfer matrix element coupling the two states.

Conjectures 2 and 3 of Ref. 1 proposed that in the thermodynamic limit ($N \rightarrow \infty$) these branch points approach the real H axis and consequently the gaps in the free energy for real H should shrink to zero. Such a shrinking would allow analytic continuation of the metastable free energy through the eigenvalue crossing, as proposed in Ref. 1.

From our numerical work, we have found that by taking a path in the complex H plane one can in fact begin on the putative metastable state on one side of a crossing and end on the metastable level on the other side. Such a path is shown in Fig. 2 for the crossing near $H = -1.0$ for $N = 9$ and $T = 1.0$. Figure 2a shows the crossing region in detail for real H . Eleven levels cross the metastable state. Figure 2b is the path taken in the complex H plane. It leaves the real H axis at $H = -0.91$ and returns at $H = -1.11$. Finally, Fig. 2c shows the analytic continuation of the free energy. The path chosen is not a special one. Any path in complex H that goes around the branch point associated with the metastable crossing will connect the appropriate levels in real H .

These results support the conjecture of Ref. 1 that the metastable free energy can be analytically continued through the crossing regions. However,

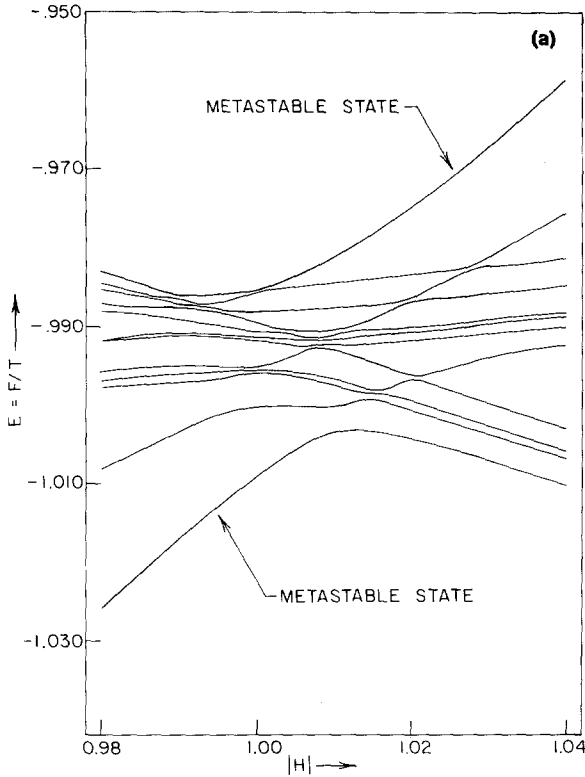


Fig. 2. Details of an energy level crossing near $\text{Re } H = -1$, for $T = 1.0$, $N = 9$ (i.e., the $2^9 \times 2^9$ transfer matrix). (a) Energy levels for $0.98 \leq -H \leq 1.04$ with $\text{Im } H = 0$. (b) A path in the complex H plane around the branch point. The path is $H = -1.01 + 0.1 \cos \pi x + i0.1 \sin \pi x$, $0 \leq x \leq 1$. (c) Real and complex parts of the free energy for the 12 levels involved in the crossing as H moves on the path shown in Fig. 2b. A path starting on the metastable level shown in the lower left-hand part of Fig. 2a ends on the metastable level in the upper right-hand part.

we find that, contrary to the other conjecture, the gap size does not shrink to zero as $N \rightarrow \infty$. In fact, the gap size changes very little with N . This can be seen in Table III for various crossings. Preliminary results also suggest that the branch points do not approach the real H axis, in agreement with approximate constancy of the gap size. The reason for both phenomena is that for large enough N each crossing consists not simply of a single state crossing the metastable state, but rather of continua which simultaneously cross it (cf. Figs. 1 and 2a).

We also observe that to the right of each gap ($|H|$ greater) the magnetization *increases* with $|H|$. This deviation from monotonically decreasing behavior also seems unchanged with N . In Section 3 we relate this non-

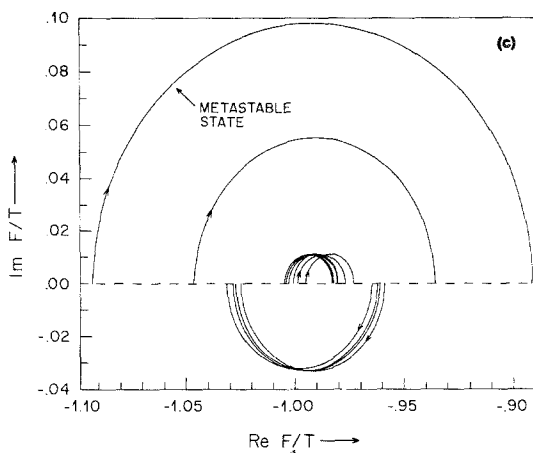
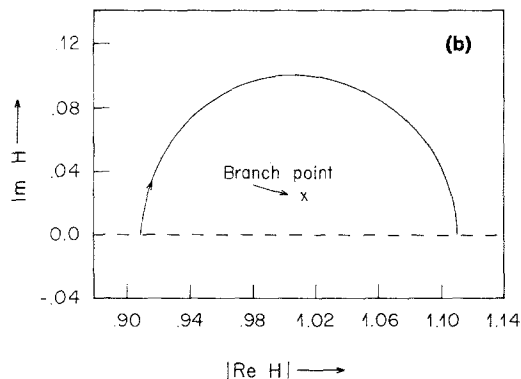


Fig. 2. Continued.

Table III. Gap Size at Various Level Crossings and for Various N for $T = 1.0^a$

$-H$	$N = 5$	$N = 7$	$N = 9$	$N = 11$
4/5	—	0.0058	0.0093	0.0099
1	0.02086	0.02207	0.02218	0.02197
4/3	0.0090	0.0111	0.0101	0.0108
2	0.1630	0.1650	0.1639	0.1640

^a First column is approximate value of $-H$ at the crossing.

concavity in the free energy to the Monte Carlo decay rate. To prepare for this section, we next investigate the crossing regions in more detail.

2.3. Location of the Crossings

For low T two states $|\mu^*\rangle$ and $|\mu'^*\rangle$ have approximately the same energy if

$$\langle \mu | L | \mu \rangle = \langle \mu' | L | \mu' \rangle \tag{8}$$

Therefore the value of H at which a crossing between the metastable state and a state of single excitation [defined by Eqs. (5) and (7)] occurs is given by

$$\langle 0 | L | 0 \rangle = \langle x | L | x \rangle \quad \text{for any } x = 1, \dots, N \tag{9}$$

The result is

$$H_c = -2J/l, \quad l = 1, 2, \dots \tag{10}$$

As noted previously, for large N , continua of states also participate in the crossings. For the single excitation crossing described by l the participating continua are those associated with k excitations ($k = 2, 3, \dots$) of a total of kl ($-$) spins. The single excitation crossings will be seen in Section 3 to be located at the same value of H as the Monte Carlo value needed for formation of an $l \times l$ critical droplet. Finally, we note that $k = 2, 3, \dots$ excitation states also participate in crossings with the metastable state that are not associated with single excitation crossings. Equating the diagonal elements of the transfer matrix of these states with the metastable matrix element [cf. Eq. (8)] gives

$$H_c = -2Jk/l, \quad k, l = 2, 3, \dots \tag{11}$$

Our numerical work confirms these values of H_c and those given by Eq. (10) for low T .

2.4. Crude Model of the Crossing

Consider only the 2×2 matrix that is the restriction of the transfer matrix to the states $|0^*\rangle$ and $|l^*\rangle$ and assume $N \exp(-2\nu l)$ is small, the latter assumption inappropriate for the thermodynamic limit but apparently useful for the range of N, T , and H that we study. The restricted transfer matrix is

$$\begin{aligned} W &= \begin{pmatrix} \langle 0^* | L | 0^* \rangle & \langle l^* | L | 0^* \rangle \\ \langle 0^* | L | l^* \rangle & \langle l^* | L | l^* \rangle \end{pmatrix} \\ &= \Lambda \begin{pmatrix} 1 & y\alpha\sqrt{N} \\ y\alpha\sqrt{N} & y^2\{1 + [2\beta(1 - \beta^{l-1})/(1 - \beta)] + (N - 2l + 1)\beta^l\} \end{pmatrix} \end{aligned} \tag{12}$$

with

$$\begin{aligned} z &= h - h_c, & h_c &= \nu H_c, & y &= \exp(-lz) \\ \alpha &= \exp(-2l\nu), & \beta &= \exp(-4\nu), & \Lambda &= \exp[N(2\nu + h)] \end{aligned} \quad (13)$$

The eigenvalues of W/Λ are

$$\frac{1}{2}(1 + uy^2) \pm \frac{1}{2}[(1 - uy^2)^2 + 4N\alpha^2y^2]^{1/2} \quad (14)$$

where

$$u = 1 + 2\beta(1 - \beta^{l-1})/(1 - \beta) + (N - 2l + 1)\beta^l \quad (15)$$

If it is assumed that $4N\alpha^2y^2$, $N\beta^l$, β , and lz are all small, then one of the energy levels $[(-1/N) \log(\text{eigenvalue})]$ associated with W goes asymptotically to the metastable level and in a range of h neither too close nor too far from the crossing is approximated by

$$E = -2\nu - h - \alpha^2/[2l(h - h_0)] \equiv -2\nu - h - \nu(\Delta F)_T \quad (16)$$

where h_0 is a real number near h_c . Equation (16) defines a two-level "level shift" function $\Delta F_T(h)$. As a function of $x \equiv -h$ ($x_0 \equiv -h_0$), $E(x)$ is a hyperbola lying above the line $E = -2\nu + x$ for $x > x_0$ and approaches the line asymptotically for large x . For $x < x_0$, E lies below $-2\nu + x$ and approaches it asymptotically. The function $(\Delta F)_T$ and the corresponding function $(\Delta F)_N$ defined below serve also as measures of the deviation of the free energy from concavity and hence from stability.

It turns out that the crossings of the transfer matrix, even though they involve far more than two levels, can be well approximated by a curve of the form (16). Values of h_0 and α are obtained from the data ("l" of course is a property of the particular crossing under investigation). The test of the validity of the quite crude estimates of this section is whether indeed the value of α obtained from the fit is approximately equal to $\exp(-2l\nu)$. In Table IV we compare the theoretical values of "l" at the two crossings $H = -2/3$ and

Table IV. The Measured l Compared to l , the Number of Inverted Spins at the Particular Crossing

$-H$	T	l	$l(H)$
2/3	1.0	2.68	3
2/3	0.714	2.86	3
2/3	0.5	2.96	3
1.0	1.25	1.90	2
1.0	1.0	1.92	2
1.0	0.714	1.96	2

-1 ($l = 3$ and 2 , respectively) with \bar{l} . To get \bar{l} we use the value $\bar{\alpha}$ obtained by fitting the energy levels to the formula (16) and then set $\bar{\alpha} = \exp(-2\bar{l}\nu)$. This in effect defines a level shift $\Delta F_N(h)$ for the numerical free energy. It will be seen that the agreement gets progressively better for lower temperatures, indicating that our very simple-minded picture does have some validity.

Expression (14) also gives some rough indication of where the branch point H_B occurs. From (14) one might expect $\text{Im } H_B \sim \alpha\sqrt{N}$, however, in preliminary checks we have found almost no N dependence at all. The α in $\text{Im } H_B$ suggests a definite temperature dependence, namely $\text{Im } H_B \sim \exp(-2l/T)$, and there are preliminary indications that this is approximately true. We can only speculate on the absence of the \sqrt{N} dependence: Perhaps the presence of the other levels affects this aspect of the model more than it does the predictions inherent in Eq. (16).

Yet another speculative step is to suppose there are branch points with imaginary part at $\exp(-2l/T)$ for $l = 1, 2, 3, \dots$, so that as $\text{Re } H \rightarrow 0$ these singularities crowd closer and more densely about the real H axis. This would lead to an essential singularity, but at the same time suggests the absence of singularity on the imaginary H axis any finite distance above $H = 0$. Thus the imaginary H axis would not be a natural boundary for the analytic continuation of the free energy.

3. DYNAMICAL ISING MODEL

We again consider an $N \times N$ lattice with periodic boundary conditions. The external field H is chosen so that the equilibrium magnetization m is close to -1.0 . The system is started with m near the metastable value $+1.0$. The dynamics is as described in Ref. 11 except that the site at which each spin flip is attempted is chosen randomly. Typically m fluctuates until it drops below some critical value, after which the system goes directly to equilibrium. For the temperatures and system sizes N at which we work the passage to equilibrium is much faster than the initial period necessary to reach the critical value. More will be said on this point later. The computer experiment is performed repeatedly with different random evolution. For those systems that have not decayed at the end of some given time³ we measure the average

³ The measured lifetimes were relatively insensitive to the time chosen. For example, four runs at $H = -1.2$, $T = 0.9$ on an 11×11 lattice gave lifetimes of 47, 43, 51, and 40 sec for cutoff times of 79, 95, 95, and 159, respectively. Variations of 10 or even 20% in lifetime (under identical circumstances but with different random numbers) were common. We considered this reasonable in view of the fact that as H and T varied we observed variations in lifetimes of more than a factor of 100. The four values of ϕ [see Eq. (17)] associated with the above measurements are 7.8, 7.7, 7.9, and 7.6, showing, as expected for a logarithm, much less variation. The total range of ϕ measured in our numerical experiments (many not reported here) was from about 2 to about 15.

magnetization during the second half of their evolution. Those that have decayed provide data for the determination of a decay rate $\Gamma(T, H)$ through the fitting of the decay times to an exponential decay law.

Γ or its inverse, the lifetime, is measured in time units of spin flip attempts per site, so that each second represents N^2 spin-flip attempts. Given Γ , let A be the expected number of spin-flip attempts before decay; thus $A = N^2/\Gamma$. For low T and moderate N we find that A is independent of N , implying a constant decay rate per unit volume. Figure 3 shows a log-log plot of lifetime (i.e., $1/\Gamma$) vs. N , confirming the volume dependence of lifetime suggested by Eq. (1). For N large enough that the time for passage to equilibrium exceeds the time of formation of the critical droplet this dependence is expected to break down. For given measured A , let

$$\phi(T, H) = T \log A \quad (17)$$

This definition is useful only if systematic dependence of ϕ on H and T is found.

Our data can be understood by interpreting ϕ to be the free energy of a critical droplet relative to the free energy of the metastable state. Moreover, the droplet free energy will be of the form $E - TS$, with E an easily identified

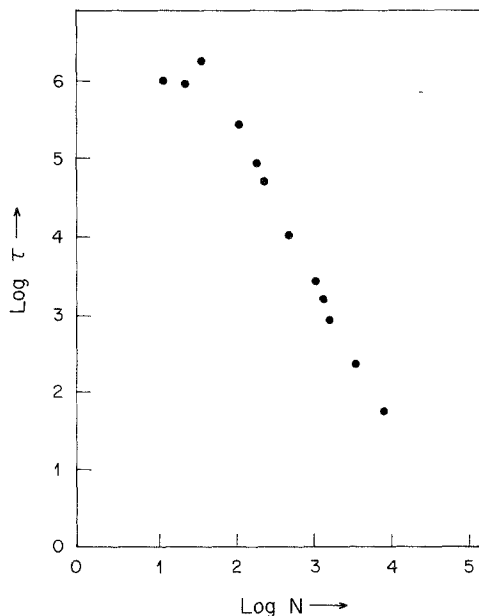


Fig. 3. Logarithm of lifetime of the metastable state on an $N \times N$ lattice vs. logarithm of N for the dynamical Ising model at $T = 0.9$ and $H = -1.1$. A least squares fit to the slope for data points involving N between 5 and 50 gives -2.0067 , in good agreement with the value 2 expected from Eq. (1).

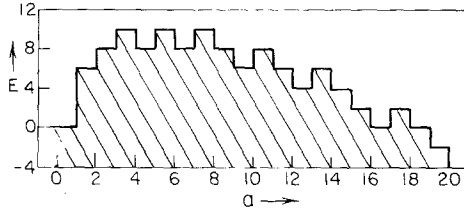


Fig. 4. The energy as a function of droplet size a for $H = -1$. Where several configurations are possible for given a , the minimum energy is plotted.

droplet energy. In the conventional description the metastable state is a free-energy minimum, with the free energy of the critical droplet the minimum barrier to be crossed to get to the stable state. The height ΔE of this barrier relative to the metastable free energy is what ought to appear as the ϕ of formula (1).

The foregoing description can be tested quantitatively against the Monte Carlo data. We first compare ΔE and ϕ . For ΔE we make the most naive possible estimate in terms of the energy cost for the creation of various configurations of reversed spins against a background of all (+) spins. Taking the Ising energy to be $E = -J \sum \sigma \sigma - H \sum \sigma$ with $J = 1$, in Fig. 4 we plot ΔE as a function of droplet size at $H = -1.0$. Thus at $H = -1.0$ the creation of two (-) spins in a background of (+) spins costs $12J - 4H = 8.0$. The maximum ΔE is 10.0, in general agreement with $\phi(T, -1.0)$ measured at various T . For example, $\phi(1.0, -1.0) = 9.0$. This agreement improves as T decreases, so that $\phi(0.833, -1.0) = 9.3$. Second, consider $\phi(T, H)$ for fixed T . If the critical droplet dominates, then $d\phi/dH$ should be determined by the number of spins reversed in the critical droplet. The barrier description implies that for $2/3 \leq |H| < 1$ this slope should be -14 (for this range of H there are seven reversed spins in the critical droplet) and should change to -6 for $|H| > 1$. These numbers are T independent except insofar as the zero- T critical droplet description is more accurate for lower T . For $T = 0.9$, Fig. 5 shows the function $\phi + 6.50|H|$ plotted against $|H|$, the linear term in $|H|$

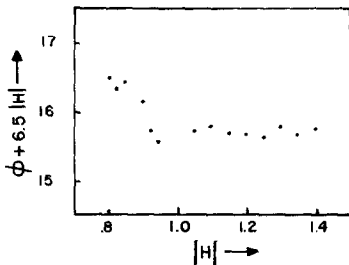


Fig. 5. Plot of $\phi(T, H) + 6.50|H|$ as a function of $|H|$ for $T = 0.9$.

having been included so as to aid in displaying the change in slope. Measured slopes of ϕ are -12.67 and -6.50 for $|H| < 1$ and $|H| > 1$, respectively, lending yet more support to the droplet model.

Finally, we make a crude analytic estimate of ϕ for small fixed H and T near zero. Assuming a square critical droplet of side j , maximizing ΔE with respect to j gives $j = 2J/|H|$. Identifying ϕ with $\max \Delta E$, we find

$$\phi = 8J^2/|H| \quad (18)$$

(Allowing for changed definitions of J and H , the same expression appears in Ref. 12.) The decay rate is then

$$\Gamma = N^2 \exp(-8J^2/|H|T) \quad (19)$$

suggesting an essential singularity for $H \rightarrow 0$. (There is a flaw in this argument which weakens considerably whatever implications it may have for conclusions about an essential singularity. Specifically, we looked at fixed H and $T \rightarrow 0$. The correct argument should involve fixed T with $H \rightarrow 0$. In this limit it seems unlikely that a square critical droplet is appropriate.)

4. RELATING TRANSFER MATRIX AND MONTE CARLO RESULTS

We have thus provided crude calculations showing that the Monte Carlo decay rate [cf. Eq. (19)] and the transfer matrix level shift [cf. Eq. (16)] are proportional to

$$\alpha^2 = \exp(-8J^2/T|H|) \quad (20)$$

This provides a link between these two seemingly different phenomena. We review the steps:

Numerical transfer matrix ΔF_N (gap size and measurement of nonconvexity of the free energy F) relates to:

Theoretical transfer matrix ΔF_T (two level), which relates to:

Theoretical Monte Carlo Γ (square droplet), which relates to:

Experimental Monte Carlo Γ .

The first connection relies on the correctness of the two-level picture and is supported by Table IV. The second connection arises because both ΔF_T for the two-level model and Γ for the square critical droplet are calculated to be proportional to α^2 [cf. Eqs. (16) and (19)]. The last connection requires the identification of ϕ with $\max \Delta E$ (cf. Figs. 4 and 5), and the relevance of the square droplet.

Having established an interpretation of the gaps, it remains to find physical values of m and F in the crossing regions. If these regions survive as N increases, it seems possible that a kind of Maxwell rule could be invented,

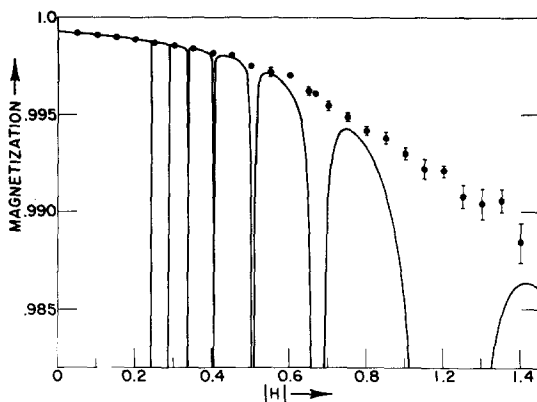


Fig. 6. Magnetization as a function of $-H$ for $T = 1$. The points are from dynamic Monte Carlo numerical experiments. The curves are from the transfer matrix eigenvalue that yields the largest magnetization at the given H .

e.g., "Let m be a linear decreasing function tangent to the magnetization curves of the metastable levels." The plausibility of some such Ansatz is suggested by Fig. 6. For small $|H|$ the transfer matrix magnetization nearly rises to the physical value between the crossings. However, after the crossing at $|H| = 2/3$ it remains below the Monte Carlo error bars. Even so, the transfer matrix values suggest a general shape and lower bound for m in this region. A further encouraging property is the N independence of m even in crossing regions, despite the increasing number of levels involved as N increases. For $N = 9$ and 11 we find agreement to the fifth decimal place for the 12 points, all in crossing regions, that we have checked.

The picture emerging from our work on the transfer matrix is that sufficiently far off the real H axis the free energy can be analytically continued to $\text{Re } H < 0$, but that near the negative real H axis there is an infinity of singularities near

$$H = (-2Jk/l) \pm i \exp(-2Jl/T), \quad k, l = 1, 2, \dots \quad (21)$$

suggesting that the point $H = 0$ is an essential singularity. On the real negative H axis the physical free energy is derived from the transfer matrix eigenvalue of largest magnetization or from some concave function defined from those eigenvalues obtained by means of a Maxwell rule or similar prescription.

5. CONCLUSIONS AND REMARKS

For the lattice sizes N studied in this paper the existence of some sort of metastability seems well established, both in the "experimental" Monte Carlo work and in the analytic behavior of the free energy as inferred from

the eigenvalues of the transfer matrix. While the conjectures of Ref. 1 have turned out to be only partially correct, the basic idea of that paper, namely analytic continuation by means of the eigenvalues, appears valid even if the singularities of the free energy remain a finite distance off the real H axis as N changes. Moreover, as verified by the Monte Carlo data, this analytic continuation seems to have something to do with the physical metastable state.

There is, however, one caveat which we feel compelled to mention. Even though we have found numerically little change in our results as N increased—from 5 to 11 for the transfer matrix and from 5 to 50 for the dynamic model—there is reason to believe that for considerably larger N , magnetizations and lifetimes might begin to change. This must surely be true for the dynamic model. For as N gets large enough, the time taken by critical droplets to grow and meet each other must exceed the time needed to form the first critical droplet. (This is because the latter time shrinks with N , while the former is determined by some sort of average spacing between droplets.) Thus for N large enough the lifetime ceases to shrink and Eq. (1) is no longer valid. This point has been made by Müller-Krumbhaar and by Stoll and Schneider.⁽⁵⁾ It is not clear whether similar limiting factors exist for the transfer matrix branch points. One feature is clear: The simple-minded estimates based on assuming that the metastable ground state is all (+) spins must break down, since the metastable magnetization is after all not exactly unity and therefore for sufficiently large N the biggest contribution to the ground state will be from states with several overturned spins. On the other hand, similar problems arise in the Lipkin model⁽¹⁾ where the replacement of a complicated superposition of states by a single state leads to estimates that are valid in the various asymptotic limits taken there. At this point the status of this problem for the Ising model transfer matrix structure is just not known.

In the event that for $N \rightarrow \infty$ free-energy singularities do not move farther from the real H axis, there would seem to be a good chance of proving that free energy can be analytically continued to $\text{Re } H < 0$ at some finite distance above the real H axis. Should, however, the singularities not remain fixed for very large N , a different view of metastability emerges: There is a region in the parameter space of N , T , and H where an empirically well-defined metastable state exists, has a reproducible magnetization and lifetime, and in which variation of N does not change these properties by much. Physically, this would mean that metastability is a finite- N (or volume) phenomenon but that this volume effect is not manifested except for very large volumes—where, in contrast to the usual situation, 10^{23} may not be “large” for many physical systems. Mathematically it would mean that the results we have been getting—the stability of branch points and volume dependence of lifetime indicated in Fig. 3—are analogous to an asymptotic

expansion with agreement improving with N for a while, but ultimately breaking down.

Again, our numerical and crude analytical computations cannot decide the issues of the foregoing paragraph. However, even if metastability is lost for $N \rightarrow \infty$, our results are still relevant to the laboratory phenomenon.

ACKNOWLEDGMENT

We are grateful to C. M. Newman for extensive and useful discussions.

REFERENCES

1. C. M. Newman and L. S. Schulman, *J. Math. Phys.* **18**:23 (1977).
2. K. Binder and H. Müller-Krumbhaar, *Phys. Rev. B* **9**:2328 (1974).
3. K. Binder, in *Phase Transitions and Critical Phenomena*, C. Domb and M. S. Green, eds. (Academic Press, New York, 1976), Vol. 5b.
4. A. Compagner, Thesis, Rijksuniversiteit te Utrecht (1972).
5. E. Stoll and T. Schneider, *Phys. Rev. A* **6**:429 (1972).
6. A. F. Andreev, *Sov. Phys.—JETP* **19**:1415 (1964).
7. M. E. Fischer, *Physics* **3**:255 (1967).
8. J. S. Langer, *Ann. Phys.* **41**:108 (1967).
9. W. Klein, D. J. Wallace, and R. K. P. Zia, *Phys. Rev. Lett.* **37**:639 (1976).
10. C. Domb, *Adv. Phys.* **9**:149 (1960).
11. D. P. Landau and R. Alben, *Am. J. Phys.* **41**:394 (1973).
12. D. Capocaccia, M. Cassandro, and E. Olivieri, *Comm. Math. Phys.* **39**:185 (1974).